The First Vanadium Oxide Nanotubes Containing an Aromatic Amine as Template

by **Fabian Bieri**, **Frank Krumeich**, **Hans-Joachim Muhr**, and **Reinhard Nesper***

Laboratory of Inorganic Chemistry, Swiss Federal Institute of Technology (ETH), Hönggerberg, CH-8093 Zürich (Tel.: +41-1 632 3069; e-mail: nesper@inorg.chem.ethz.ch)

Dedicated to the memory of Prof. *Luigi M. Venanzi*

A new vanadate has been prepared in high yield by reacting vanadium(V) triisopropoxide and 3-phenylpropylamine in solution, followed by hydrolysis and hydrothermal treatment of the intermediate product. For the first time, an aromatic amine has successfully been applied as structure-directing template for the synthesis of vanadium oxide nanotubes. Scanning electron microscopy (SEM) and transmission electron microscopy (TEM) images demonstrate the tubular morphology of the phenylpropylamine vanadium oxide nanotubes obtained. The size and structure are similar to that of vanadium oxide nanotubes formed with aliphatic amines. The tube walls comprise layers of vanadium oxide with the organic template intercalated in between. The interlayer distance is *ca.* 2.1 nm, and the structure of the VO_x layers can be described by a square lattice with $a \approx 0.61$ nm. Furthermore, the TEM investigation has revealed the presence of many defects in the wall structure.

Introduction. – The anisotropic structure of tubular materials, such as the well-investigated nanotubes of carbon [1], WS_2 [2], and TiO_2 [3], is linked to interesting physical and chemical properties [4]. At present, such materials are the focus of worldwide investigations because of their outstanding properties that open up visions of various applications as multifunctional nanodevices [5]. First achievements in realizing the promising potential of nanotubes have already been obtained, in particular for carbon nanotubes that can be applied, *e.g.*, to hydrogen storage and as field emitters [4]. Further examples of nano phases that crystallize with a tubular morphology are the vanadium oxide nanotubes (VO_x-NTs) [5–9], which, moreover, contribute to the multitude of vanadium oxide derivatives [10][11]. The VO_x-NTs are prepared by a sol-gel reaction followed by hydrothermal treatment from vanadium(V) alkoxides and primary monoamines ($C_nH_{2n+1}NH_2$, with $4 \leq n \leq 22$). After washing, the product is phase-pure and consists of VO_x-NTs only [7]. Besides alkoxides, V_2O_5 and $VOCl_3$ are useful as vanadium precursors that, in addition, provide an easy and cheap access to large quantities of VO_x-NTs [12]. In addition, α,ω-diamines ($H_2N[CH_2]_nNH_2$ with $12 \leq n \leq 20$) can alternatively be used as structure-directing templates [13]. However, in spite of the wide range of applicable primary monoamines and diamines, synthesis of tubes has been accomplished only with aliphatic amines so far. This restriction has been overcome now by the successful preparation of the first VO_x-NTs with an aromatic template, namely 3-phenylpropylamine. The synthesis and the results of the structural characterization of this new type of VO_x-NT will be presented in this paper.

Results and Discussion. – 3-Phenylpropylamine vanadium oxide nanotubes, in the following abbreviated as PPA-VO_x-NTs, have been synthesized in the same way as the VO_x-NTs containing aliphatic amines [7]: a vanadium(V) alkoxide and the amine are reacted in an EtOH solution, and, after hydrolysis and aging, a hydrothermal treatment at 180° results in formation of a black material. Scanning electron microscopy (SEM) images (*Fig. 1*) as well as transmission electron microscopy (TEM) images at low

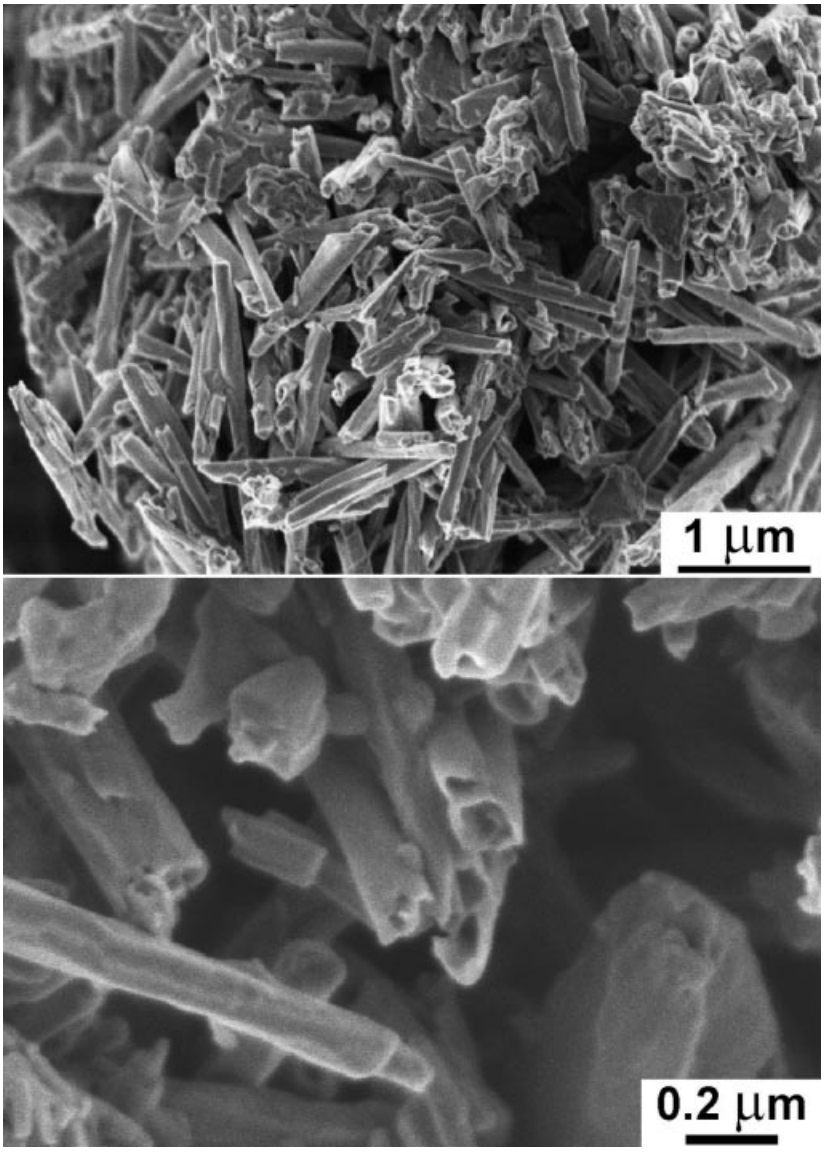

Fig. 1. *SEM Images of 3-phenylpropylamine vanadium oxide nanotubes* (PPA-VO_x-NTs). a) *Survey.* b) *Enlarged view on tube ends, demonstrating that the tube tips are open.*

magnification (*Fig. 2*,*a*) demonstrate that nanotubes indeed are the main product. Besides that, a by-product is present. No crystal facets are distinguishable, and the material appears to be amorphous according to electron diffraction. In general, the PPA-VO_x-NTs are 0.5 – 5 μm long and have an outer diameter between 50 and 150 nm. A whole PPA-VO_x-NT, which is relatively short (length *ca*. 0.7 μm) and has open ends, is shown in *Fig. 2*,*b*. Only NTs with open tips have been found so far (*Figs. 1*,*b*, and *2*).

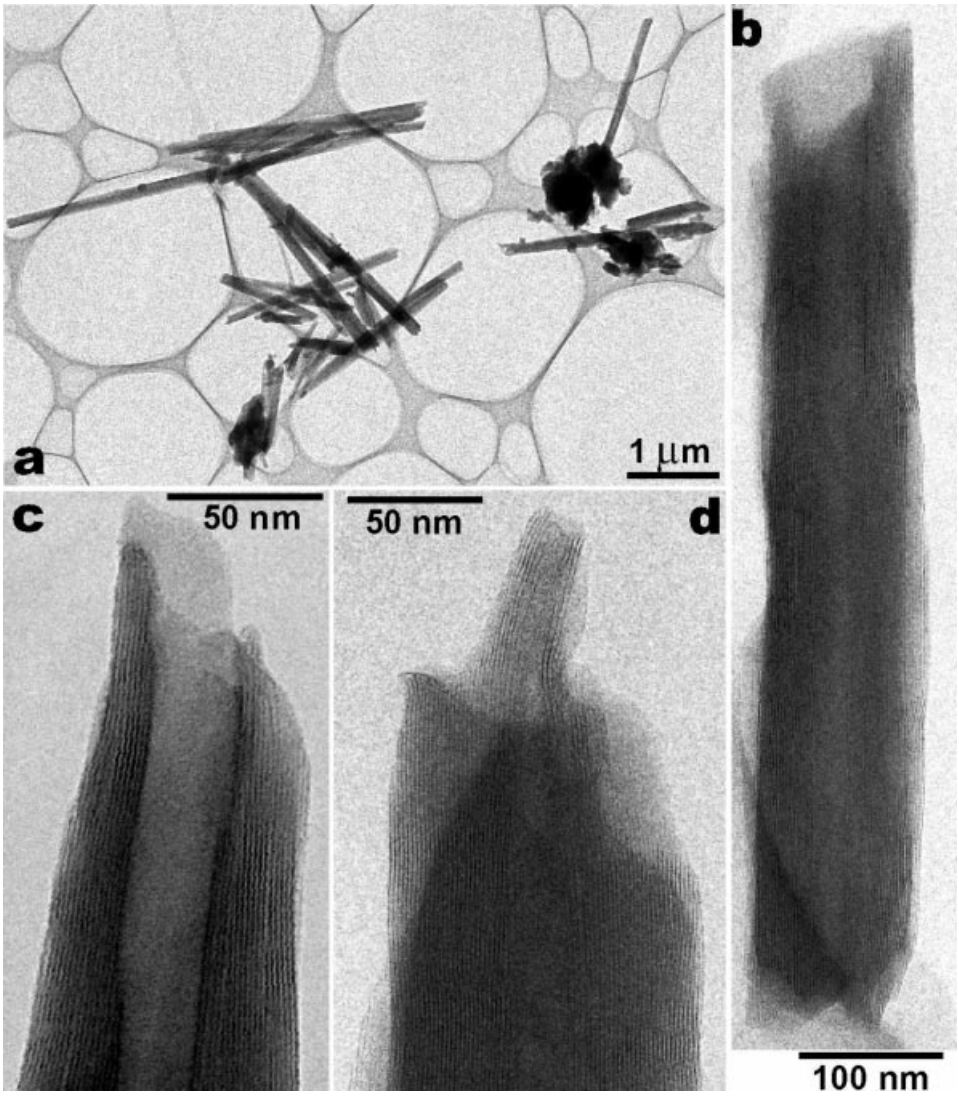

Fig. 2. *TEM Images of PPA-VO_x-NTs in longitudinal projection*. a) *Survey at low magnification*. Isolated tubes are predominant. Some particles of an amorphous by-product are present. b) *Single NT with open ends*. c and d) *Ends of two tubes at higher magnification*. The tube walls appear as alternating lines with dark and bright contrast. The layers forming the thick tube walls in *d* terminate at several sites, leading to a smaller tube tip.

The tube walls comprise a layered structure. In TEM images (*Figs. 2* and *3*), the structure inside the tube walls appears as parallel dark and bright strips, which are arranged alternately and equidistantly with respect to each other. It has been unambiguously established by elemental mapping in the case of VO_x-NTs with aliphatic templates [7][9] that the dark contrasts indicate VO_x layers while the bright ones correspond to amine layers.

For an unambiguous discrimination between PPA-VO_x-NTs built from closed concentric VO_x cylinders and NTs built from scrolls of VO_x layers, an observation along the tube axis is necessary. In cross-sectional images (*Fig. 3*), most parts of the structure

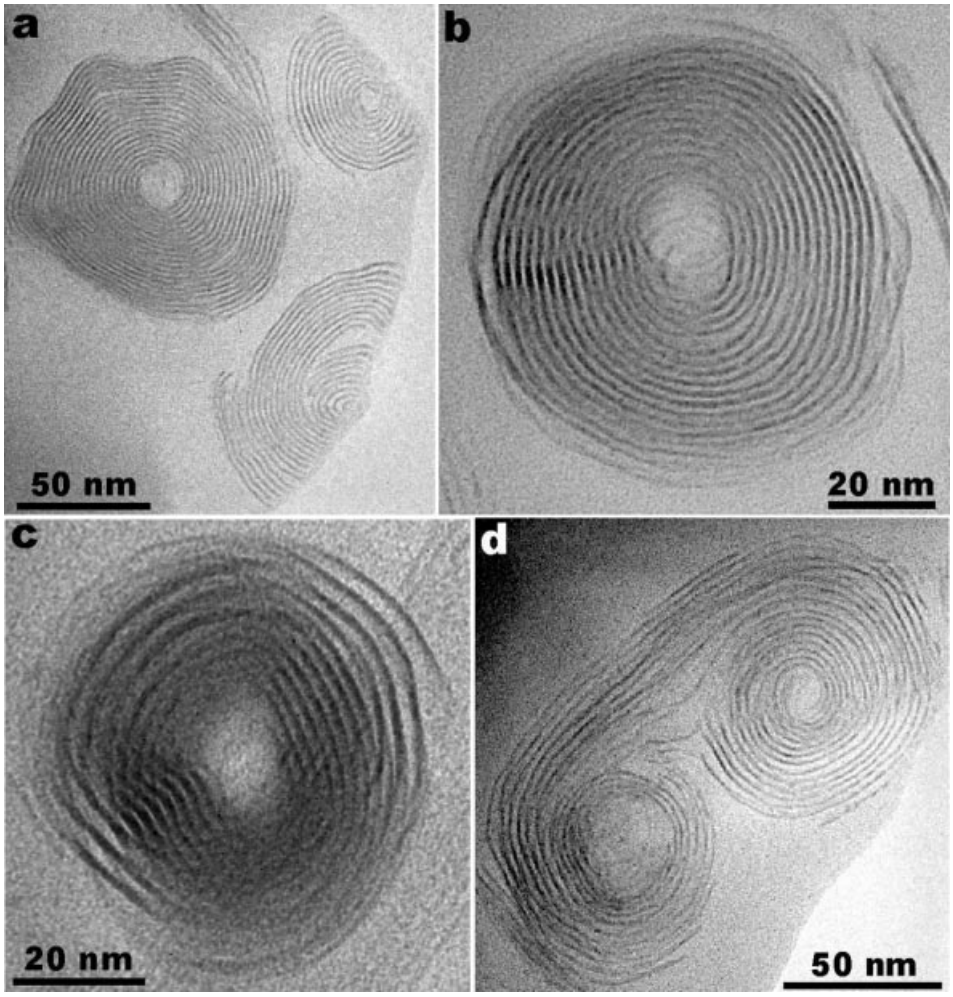

Fig. 3. *Cross-sectional TEM images of PPA-VO_x-NTs.* a) *A thick tube* (*ca.* 20 layers) *and tube fragments located in a thin area close to the hole in the TEM specimen*. b) *In the central part of this tube, dark layers overlap, indicating defects in the direction of observation*. c) *Tube with partly blurred contrast.* The wall structure is distorted; the interlayer distance differs significantly in different parts of the tube. d) *A pack of VO_x layers is scrolled at both sides, resulting in a double tube.*

inside the wall can clearly be observed in thin specimen regions. Unfortunately, it is impossible to discern the positions of the VO_x layers in all regions of the tube walls due to a blurring of their contrast at some sites. However, the dangling ends of the VO_x layers, often recognizable in the tube core as well as at its outer surface, clearly point to the presence of scrolls (*Fig. 3*,*a*). While, in the case of VO_x-NTs with aliphatic amines, closed cylinders have been found in addition to scrolls and intermediate arrays [9], only scrolls and disordered arrangements have been observed in the PPA-VO_x-NTs to date (*Fig. 3*).

The average distance between the parallel VO_x layers in the tube walls gives rise to certain reflections in reciprocal space. As a result, strong reflections at low 2Θ values appear in the XRD pattern (*Fig. 4*,*a*), and a row of sharp reflections with narrow distances close to the direct beam are in the electron-diffraction pattern (*Fig. 4*,*b*) [7]. From the position of these reflections in the XRD pattern, the distance between the VO_x layers has been determined to be *ca.* 2.1 nm. A smaller value of *ca.* 1.85 nm has been measured by electron diffraction. A similar discrepancy was also observed in the case of aliphatic VO_x-NTs and is most likely caused by a shrinkage of the inter-layer distance induced by the electron beam in the microscope vacuum [7].

Further low-intensity *Bragg* reflections, which are present in the diffraction patterns (*Fig. 4*), provide information about the crystalline structure inside the multilayer VO_x walls. As in the case of VO_x-NTs with aliphatic templates [7], these reflections can be assigned to a square lattice with an edge length corresponding to *ca.* 0.615 nm in real space. As a result, the structure can be approximately described by a unit-cell with a tetragonal shape ($a = b \approx 0.615$ nm, $c \approx 2.1$ nm). This is analogous to the aliphatic VO_x-NTs [7]. In fact, corresponding *hk*0 reflections of all VO_x-NTs appear in nearly the same positions in the reciprocal space independently of the type of template incorporated inside the tube walls [7]. This observation strongly supports the

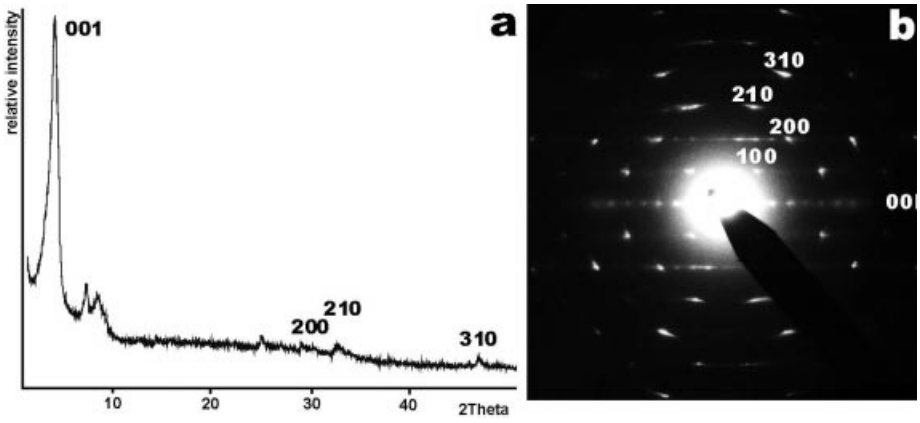

Fig. 4. a) *Powder X-ray and* b) *electron diffraction pattern of PPA-VO_x-NTs.* The indices are assigned to the reflections on the basis of a cell with a tetragonal shape: $a = b \approx 0.615$ nm, $c \approx 2.1$ nm. The spots in *b* reveal the nearly single crystalline character of the VO_x layer structure, but they are somewhat blurred because of disorder and bending. As in the case of aliphatic templates [7], the angle between the *a**-axis and the row of 00*l* reflections (*c**-axis) is 45°.

assumption that the basic structure underlying the VO_x layers in the PPA-VO_x-NTs is the same as in the VO_x-NTs with aliphatic amines. At present [14], all experimental evidence points to a close structural relationship of the VO_x layer in the tubular vanadates to that present in BaV_7O_{16} [15].

The inter-layer distance of *ca.* 2.1 nm is approximately twice the length of the 3-phenylpropylamine molecules, which are *ca.* 1.0 nm long. This indicates a double layer of 3-phenylpropylamine molecules building up the organic layer of the tube walls (*Fig. 5*). Remarkably, the molecules that point into opposite directions obviously do not overlap each other in the center of the amine layers. Therefore, interactions between the π electrons of the Ph groups of the molecules seem not to be utilized. However, the PPA-VO_x-NTs appear to have a considerable stability, which is

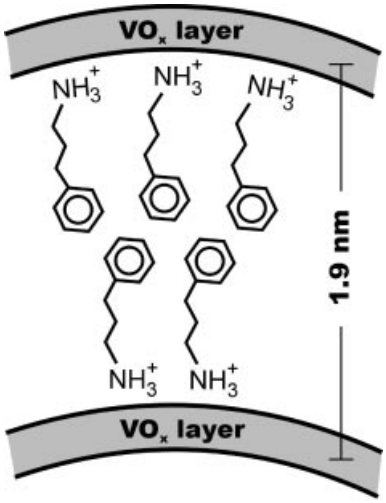

Fig. 5. *Schematic representation of the layer structure inside the tube walls.* The protonated 3-phenylpropylamine molecules have a length of *ca.* 1 nm and thus do not overlap in the center of the organic layer.

comparable to that of aliphatic VO_x-NTs. It should be mentioned that tubes were not obtained with other aromatic amines, such as methylnaphthylamine or xylylenediamine. Consequently, it is likely that the C chain of the aliphatic propyl group is necessary for the reaction to occur. Since the N-atoms of the amine molecules are protonated in the aliphatic tubes according to XPS results [7], a high basicity of the NH_2 group seems to be an important prerequisite for the tube formation. In 3-phenylpropylamine, the distance between the NH_2 group and the Ph group, which are attached to opposite ends of the propyl group, decreases the electron-withdrawing effect of the latter. This results in a rather large basicity of the NH_2 group that is nearly comparable to that of aliphatic amines. Other amines with reduced basicity due to the presence of an electron-withdrawing group, *e.g.*, the amino acids alanine, glycine, and cysteine, also failed to support tube formation. Steric effects obviously limit the applicability as templates to primary amines.

The broadening of the signals in the XRD pattern already hints at the presence of disorder, and defects of the tubular morphology are recognizable in the SEM images

(*Fig. 1*). Besides nearly perfect NTs that have a rotationally symmetric shape, there are distorted tubes that have bent fragments attached to them. This seems to be an indication for a perturbed scrolling of a plate-shaped intermediate (see below). The low degree of order inside the tube walls is uncovered by TEM images taken in longitudinal (*Fig. 2*) and cross-sectional projection (*Fig. 3*). In *Fig. 2*, *c*, the thickness of the tube walls decreases close towards the open tube end because the number of VO_x layers decreases. This effect is more pronounced in the tube in *Fig. 2*, *d*. A large fraction of layers is missing at the outer surface of the tube tip leading to a smaller nanotube fragment emerging from the center of the larger tube. The presence of disorder in the PPA-VO_x-NTs in projection along the tube leads to overlapping or even to blurring of the layer contrast (*Fig. 3*, *b* and *c*). The VO_x layers of two differently structured sections can be discerned in the core of the tube shown in *Fig. 3*, *b*. The observation of scrolls strongly suggests a mechanism for the formation of these tubes *via* scrolling of an intermediately formed lamellar product. The bending of this sheet-like structure apparently occurs during the final hydrothermal treatment and gives rise to the tubes. This assumption is further supported by the arrangement in *Fig. 3*, *d*, where a pack of layers is scrolled at two sides, leading to a double scroll. However, the high frequency of defects observed here demonstrates that the scrolling of the sheets and the build-up of the tube walls proceeds in an imperfect and disturbed way.

Conclusions. – PPA-VO_x-NTs are the first vanadium oxide nanotubes to utilize an amine with an aromatic group as the structure-directing template and incorporate it into the tube walls between the VO_x layers. These novel tubes constitute an important addition to the family of vanadate nanotubes that, up to now, has included members accessible with aliphatic amines only. The tubular morphology as well as the layered wall structure of the PPA-VO_x-NTs and the aliphatic VO_x-NTs are very similar. Remarkably, the underlying structural principle appears to be very flexible as indicated by the observed multitude of closely related vanadate derivatives, which can be obtained under very similar synthesis conditions. These findings strongly suggest that these tubular vanadium oxide phases develop a rather optimized structure with considerable kinetic stability.

We thank Dr. *H. Jaksch* (*LEO*, Oberkochen) for performing the SEM investigation. Generous financial support by the ETH-Zurich (TEMA grant) is gratefully acknowledged.

Experimental Part

Synthesis. A soln. of vanadium(V) triisopropoxide (*ABCR*) and 3-phenylpropylamine (*Fluka*) (molar ratio 2:1) in abs. EtOH (3 ml/g vanadium precursor) is stirred under an inert atmosphere (1 h). The resulting yellow soln. of the alkoxide-amine adduct was hydrolyzed with H_2O (5 ml/g vanadium precursor) under vigorous stirring. An orange composite of surfactant and hydrolyzed vanadium oxide components were obtained after aging (12 h). The hydrothermal reaction of this composite in an autoclave (180°, 6 d) results in a black product, which is washed with EtOH and hexane and dried at 80° (1 d) under vacuum.

Structural Characterization. X-Ray powder-diffraction (XRD) patterns were measured in transmission mode (0.3-mm glass capillaries, CuK_{α_1} radiation) on a *STOE STADI-P2* diffractometer equipped with a position-sensitive detector (resolution *ca.* 0.01° in 2Θ). Scanning electron microscopy (SEM) images were recorded on a *Gemini 1530* field emission microscope (*LEO*, Oberkochen), operated at low acceleration voltage (V_{acc} = 1.1 kV), which permits investigation of the as-synthesized, uncoated sample without charging problems. Transmission electron microscopy (TEM) investigations were performed on a *CM30* microscope equipped with

SuperTwin objective lens (*Philips*, Eindhoven; cathode: LaB_6). For the investigation of the longitudinal structure, the nanotube material was deposited onto a perforated C foil supported on a Cu grid. To observe the structure perpendicular to the tube axis, a modified cross-sectional preparation technique was applied as described in [9][16].

REFERENCES

[1] P. M. Ajayan, *Chem. Rev.* **1999**, *99*, 1787.
[2] R. Tenne, M. Homyonfer, Y. Feldman, *Chem. Mater*. **1998**, *10*, 3225.
[3] T. Kasuga, M. Hiramatsu, A. Hoson, T. Sekino, K. Niihara, *Langmuir* **1998**, *14*, 3160.
[4] C. N. R. Rao, B. C. Satishkumar, A. Govindaraj, M. Nath, *ChemPhysChem.* **2001**, *2*, 78.
[5] R. Nesper, H.-J. Muhr, *Chimia* **1998**, *52*, 571.
[6] M. E. Spahr, P. Bitterli, R. Nesper, M. Müller, F. Krumeich, H.-U. Nissen, *Angew. Chem.*, *Int. Ed*. **1998**, *37*, 1263.
[7] F. Krumeich, H.-J. Muhr, M. Niederberger, F. Bieri, B. Schnyder, R. Nesper, *J. Am. Chem. Soc*. **1999**, *121*, 8324.
[8] H.-J. Muhr, F. Krumeich, U. P. Schönholzer, F. Bieri, M. Niederberger, L. J. Gauckler, R. Nesper, *Adv. Mater*. **2000**, *12*, 231.
[9] F. Krumeich, H.-J. Muhr, M. Niederberger, F. Bieri, R. Nesper, *Z. Anorg. Allg. Chem.* **2000**, *626*, 2208.
[10] P. Y. Zavalij, M. S. Wittingham, *Acta Crystallogr.*, *Sect. B* **1999**, *55*, 627.
[11] T. Chirayil, P. Y. Zavalij, M. S. Wittingham, *Chem. Mat*. **1998**, *10*, 2629.
[12] M. Niederberger, H.-J. Muhr, F. Krumeich, F. Bieri, D. Günther, R. Nesper, *Chem. Mat*. **2000**, *12*, 1995.
[13] F. Krumeich, H.-J. Muhr, M. Niederberger, F. Bieri, M. Reinoso, R. Nesper, in 'Nanophase and Nanocomposite Materials III', Eds. S. Komareni, J. C. Parker, H. Hahn, MRS Symposium Proceedings, Warendale, 2000, Vol. 581, pp. 393 – 398.
[14] F. Krumeich, M. Wörle, F. Bieri, R. Nesper, Contribution to the 8th Conference on Solid State Chemistry, Oslo, 2001.
[15] X. Wang, L. Liu, R. Bontchev, A. J. Jacobson, *Chem. Commun*. **1998**, 1009.
[16] E. Müller, F. Krumeich, *Ultramicroscopy* **2000**, *84*, 143.

Received June 6, 2001